Review of Scientific Instruments

RESEARCH ARTICLE | AUGUST 30 2023

Correlation between reference point indentation and mechanical properties of 3D-printed polymers

Siyuan Pang ; Iwona Jasiuk

Rev. Sci. Instrum. 94, 085118 (2023)
https://doi.org/10.1063/5.0149701

Review of Scientific Instruments ARTICLE pubs.aip.org/aip/rsi

Correlation between reference point indentation and mechanical properties of 3D-printed polymers

Cite as: Rev. Sci. Instrum. 94, 085118 (2023); doi: 10.1063/5.0149701
Submitted: 7 March 2023 • Accepted: 7 August 2023 •
Published Online: 30 August 2023

Siyuan Pang and Iwona Jasiuk[a)]

AFFILIATIONS

Department of Mechanical Science and Engineering, University of Illinois at Urbana Champaign, 1206 West Green Street, Urbana, Illinois 61801, USA

[a)]**Author to whom correspondence should be addressed:** ijasiuk@illinois.edu. **Telephone:** (217) 333-9259. **Fax:** 217-244-6534

ABSTRACT

Reference point indentation (RPI) is a novel experimental technique designed to evaluate bone quality. This study utilizes two RPI instruments, BioDent and Osteoprobe, to investigate the mechanical responses of several 3D-printed polymers. We correlated the mechanical properties from a tensile test with the RPI parameters obtained from the BioDent and OsteoProbe. In addition, we tested the same polymers five years later (Age 5). The results show that for Age 0 polymers, the elastic modulus is highly correlated with average unloading slope (r = 0.87), first unloading slope (r = 0.85), bone material strength index (BMSi) (r = 0.85), average loading slope (r = 0.82), first indentation distance (r = 0.79), and total indentation distance (r = 0.76). The ultimate stress correlates significantly with first unloading slope (r = 0.85), average unloading slope (r = 0.83), BMSi (r = 0.81), first indentation distance (r = 0.73), average loading slope (r = 0.71), and total indentation distance (r = 0.70). The elongation has no significant correlation with the RPI parameters except with the average creep indentation distance (r = 0.60). For Age 5 polymers, correlations between mechanical properties and RPI parameters are low. This study illustrates the potential of RPI to assess the mechanical properties of polymers nondestructively with simple sample requirements. Furthermore, for the first time, 3D-printed polymers and aged polymers are investigated with RPI.

I. INTRODUCTION

Reference point indentation (RPI) is a technique that applies micro-indentation on the sample's surface to obtain force and displacement data.[1,2] BioDent and OsteoProbe (Active Life Scientific, Inc., CA, USA) are two instruments that utilize RPI but have different characteristics and outputs. BioDent is composed of a testing probe and a reference probe.[3] The reference probe penetrates material of interest with a pre-load. Then, the testing probe indents the region cyclically and records displacement–force curves. Nine parameters are calculated from the load–displacement curves, as shown in Fig. 1, and summarized in Table I.

In a similar concept but different manner to Biodent, OsteoProbe establishes a reference point through pre-loading utilizing a single probe. Once the probe penetrates to a certain depth, it indents the material, and the displacement of the tip is measured.[1] The resulting bone material strength index (BMSi) is calculated using the following equation:[5]

$$\mathrm{BMSi} = 100 \cdot \frac{\text{Indentation distance increase into PMMA}}{\text{Indentation distance increase into sample}}. \quad (1)$$

Unlike BioDent, which necessitates *in vitro* sample preparation, OsteoProbe enables *in vivo* testing for clinical applications.[6–8] Furthermore, OsteoProbe involves a significantly faster loading rate of 120 000 N/s, while BioDent performs loading at 40 N/s.[9] On the other hand, BioDent offers more user-defined controls, allowing adjustments for the reference probe, preconditions, loading forces, and loading cycles. BioDent also provides the opportunity to obtain more detailed material information through various output parameters, whereas OsteoProbe gives only one parameter. Thus, in this study, we investigate the outputs from both devices to offer deeper insights into material characterization using the RPI.

The BioDent and OsteoProbe are devices designed to measure bone quality. However, the outputs do not directly give mechanical properties. Many studies[3,9–13] have investigated how RPI

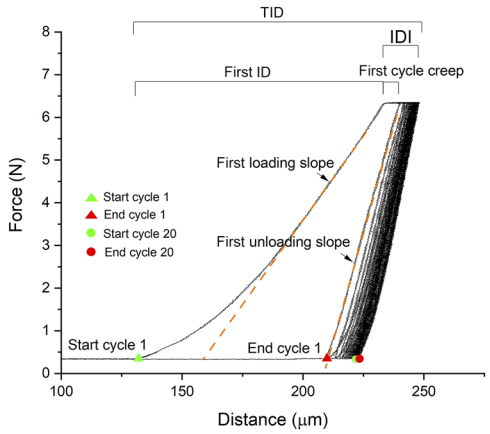

FIG. 1. Displacement–force curves generated by BioDent, showing the BioDent parameters. TID denotes a total indentation distance, IDI represents an initial indentation distance, while the first ID indicates an indentation distance due to the first cycle.

TABLE I. BioDent output parameters.[4]

BioDent parameters	Description
First ID	First cycle indentation distance
IDI	Indentation distance increase
TID	Total indentation distance
First CID	First cycle creep indentation distance
AvCID	Average creep indentation distance
First US	First cycle unloading slope
AvUS	Averaged unloading slope
AvLS	Averaged loading slope
AvED	Averaged energy dissipated

parameters relate to bone material properties *in vivo* and *in vitro*. Most studies have used RPI to assess bone fracture toughness because of its clinical importance. Approximately 40 vol. % of bone consists of collagen, a biopolymer.[14] Given the potential of the RPI technique as an indicator of bone material properties, there is a significant interest in investigating its applicability for assessing the mechanical properties of polymeric materials. Traditional approaches, such as tensile and compressive tests, have been extensively employed to study the properties of polymers.[15,16] However, RPI is a nondestructive technique that offers advantages over traditional mechanical tests. It requires simple sample geometry, is easily set up for testing, and avoids sample damage or alteration during evaluation. RPI technique uses microscale tips compared to Rockwell and Vickers hardness tests that involve much larger tips to perform indents at a larger scale. Such microscale measurements can provide new insights into polymer properties. Several prior studies have used RPI to test polymers. The correlation of RPI with hardness was studied by Ly *et al.*[17] They found a significant correlation of BMSi with Vickers hardness (r = 0.94) and Rockwell hardness (r = 0.93). Tang *et al.*[18] correlated BMSi with shore hardness (r = 0.98) and elastic modulus (r = 0.98) obtained from tensile tests. However, the RPI parameters have not been correlated with other mechanical properties of polymers.

To enhance the novelty of this study, we opted to employ 3D-printed polymers to explore the correlation between RPI and the mechanical properties of polymers. In recent years, 3D-printed polymers have gained significant traction and found use in broad commercial applications.[19] Distinct from conventional polymer manufacturing methods, a layer-by-layer fabrication process of 3D-printed materials enables easy creation of customized geometries. However, this layered construction also introduces orientation-dependent mechanical properties.[20] Moreover, polymers undergo aging processes that progressively degrade their mechanical properties.[21] No prior studies have investigated RPI on freshly 3D-printed polymers or aged polymer samples. Therefore, delving deeper into the properties of 3D-printed polymers using the RPI technique holds significant scientific value and should provide new insights.

This paper investigates 3D-printed polymers and aims to correlate the RPI parameters obtained from BioDent and OsteoProbe with the elastic modulus, ultimate stress, and elongation at break obtained from tensile tests. Nine different polymers were 3D printed using several additive manufacturing techniques. In addition, we performed RPI and tensile tests on 3D-printed polymers stored in the laboratory for five years to investigate the property changes due to aging. Thus, for the first time, this study correlates the RPI parameters with the mechanical properties of 3D-printed polymers and investigates aged polymers with RPI techniques.

II. MATERIALS AND METHODS

A. 3D-printed polymers

Nine different polymers were 3D printed in 2016 (Age 0): PA2200, ABS-M30, polycarbonate (PC), PC-ABS, VeroWhite, FullCure720, TangoBlack, ProtogenWhite, and WaterClear Ultra. The materials were 3D printed in the Rapid Prototyping Lab at the University of Illinois at Urbana-Champaign using four additive manufacturing technologies. The 3D printers, printing techniques, and thickness layer for each polymer type are listed in Table II. The bulk sample dimension employed in this study was 25.4 × 25.4 × 50.8 mm^3. The samples were 3D printed in these dimensions, and no polishing was done after printing. The layer thickness for the different materials was obtained from product specification sheets; however, it is important to note that these values are estimates and may vary depending on specific printing conditions. Among all materials, PA2200 was the only powder-based material in this study, with an average particle size of 56 μm.[22] ABS-M30, WaterClear, FullCure720, and VeroWhite are amorphous acrylic polymers. ProtogenWhite is an epoxy resin, and TangoBlack is an elastomer material. TangoBlack exhibits high elongation but low strength, while FullCure720 demonstrates superior mechanical properties regarding tensile ultimate strength and flexure strength. ABS-M30, on the other hand, exhibits the highest hardness among the materials studied. These selected materials offer a wide range of mechanical properties that effectively fulfill the objectives of this study.[18] The mechanical properties of these materials, investigated in this study by tensile tests, are reported in Sec. III. The materials printed by PolyJet initially arrived with sacrificial materials that had

TABLE II. Summary of 3D-printed polymers, printing techniques, and layer thickness used in this study.

No.	Polymer materials	Printing techniques	Layer thickness, mm
1	PA2200 (PA12)	Selective laser sintering (SLS)	0.10
2	ABS-M30	Fused filament fabrication (FDM)	0.35
3	Polycarbonate (PC)	FDM	0.25
4	PC-ABS	FDM	0.30
5	VeroWhite	PolyJet	0.02
6	FullCure720	PolyJet	0.03
7	TangoBlack	PolyJet	0.02
8	ProgenWhite	Stereolithography (SLA)	0.05
9	WaterClear Ultra	SLA	0.10
10	Polymethyl methacrylate (PMMA)	N/A	N/A

not been removed. These sacrificial materials were removed manually and rinsed with water to ensure the complete elimination of any residue. Polymethyl methacrylate (PMMA), which was not 3D printed, was also tested and used for calibration for RPI. The batch of polymers, printed in 2016, underwent proper storage measures. The specimens were sealed in plastic bags and stored in a controlled environment. Occasional exposure to light has occurred during the storage period. The storage conditions included a constant temperature of 20 °C and a humidity level of 20%. This controlled storage environment was maintained over five years until the polymers reached an age of five years in 2021.

We collected the mechanical properties of Age 0 polymers from TechSheets published by 3D-printing companies. We tested each polymer type only once at Age 0 in our lab, which was insufficient to conclude statistical significance. Furthermore, FullCure720 was no longer available to us. Thus, we report Age 0 tensile properties from TechSheets published by Stratasys.[23] The Age 0 properties we measured were very close to the values in TechSheets. Therefore, we assume that the mechanical properties in TechSheets can represent the properties of Age 0 polymers. Elastic modulus, ultimate tensile stress, and tensile elongation at break were collected for Age 0 polymers. The mechanical properties of Age 5 polymers were determined by the tensile test using an MTS Insight electromechanical testing system with a 2000 N load cell (MTS system Corp., Eden Prairie, MN). Tensile tests were done on 3D-printed samples in the printing direction. RPI was performed on Age 0 and Age 5 samples with indentation forces applied perpendicular to the printing direction.

B. Reference point indentation—BioDent

The Age 0 and Age 5 polymers were indented by BioDent reference point indentation (Active Life Scientific, CA, USA) using the BP2 probe type. The BP2 probe, made of 440C stainless steel, features a semi-sharp reference tip with a blunt cylindrical end, while the test probe is characterized by a 90° conical shape with a base radius of 370 μm and an end tip radius of 2.5 μm.[8] The probe size is smaller than the PA2200 grain size (~56 μm) and the pore size (~10 μm on average).[21] Images of the Biodent tip and the indenting point on an Ultra Clear polymer sample are shown in Fig. 2. Each sample was placed on the BioDent stage to perform indents. Indentation was conducted on samples with a 25.4 mm thickness, which greatly exceeds the required sample thickness for RPI (ten times thicker than the largest indenting depth). After the reference probe touched the sample surface, the testing probe was indented on a material with 6 N force, 20 indenting cycles, and 2 Hz frequency at a touchdown force threshold of 0.1 N. This setup followed the RPI testing procedure study of Setters and Jasiuk.[24] During the cyclic loading and unloading, the displacements of the testing probe were measured. Five indentations were

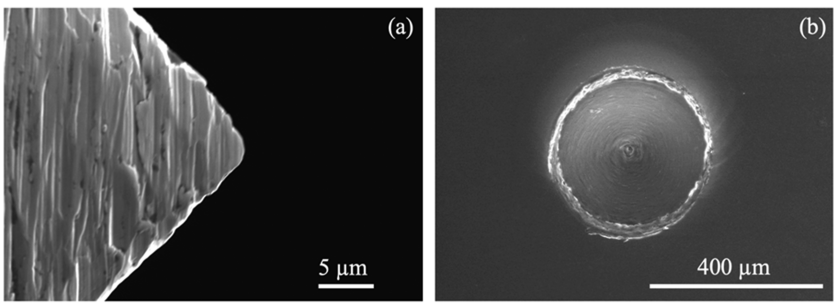

FIG. 2. Environmental scanning electron microscopy images. (a) Biodent test probe tip with a radius of 2.5 μm. (b) The indented point by Biodent on a sample of UltraClear polymer.

performed on each sample at different locations with spacings larger than 2 mm.

C. Reference point indentation—OsteoProbe

The OsteoProbe indentation (Active Life Scientific, CA, USA) was also used to perform micro-indents on Age 0 polymer surfaces. The 90° conical tip is made of 440C stainless steel, and the tip radius is less than 10 μm.[5] OsteoProbe was held perpendicular to the top surface of a sample. The probe established a reference point with a 10 N compression force. Once the reference point was reached, the probe further indented into the polymer with a 30 N force and measured the distance. After indenting the reference material, the bone material strength index (BMSi) was determined as 100 times the ratio of indentation distance increase (IDI) from reference material (PMMA) to IDI of the polymer sample using Eq. (1).[5] Ten indentations were performed on each polymer sample, and the spacing between indents was larger than 2 mm.

D. Tensile testing

Tensile tests (Instron, MA, USA) were carried out on Age 5 samples. Tensile samples were designed and printed according to the tensile test's ASTM D638 standard plastic geometry. After vertically mounting a sample onto the grips, an extensometer was put in the middle of the sample gauge to measure the strain. A 100 kN load cell with a 4 mm/min strain rate was used to perform the tensile tests. Engineering stress vs engineering strain curve was obtained from the tensile test data. The elastic modulus was calculated from the slope of the linear region of the stress–strain curve. The ultimate stress was determined at the maximum stress point. The elongation was obtained at the strain at which the sample failed.

E. Statistical analysis

Five indents were performed on each sample using BioDent on Age 0 and Age 5 polymers. Ten indents were done using OsteoProbe on Age 0 polymers. Three samples of each Age 5 polymer were tested

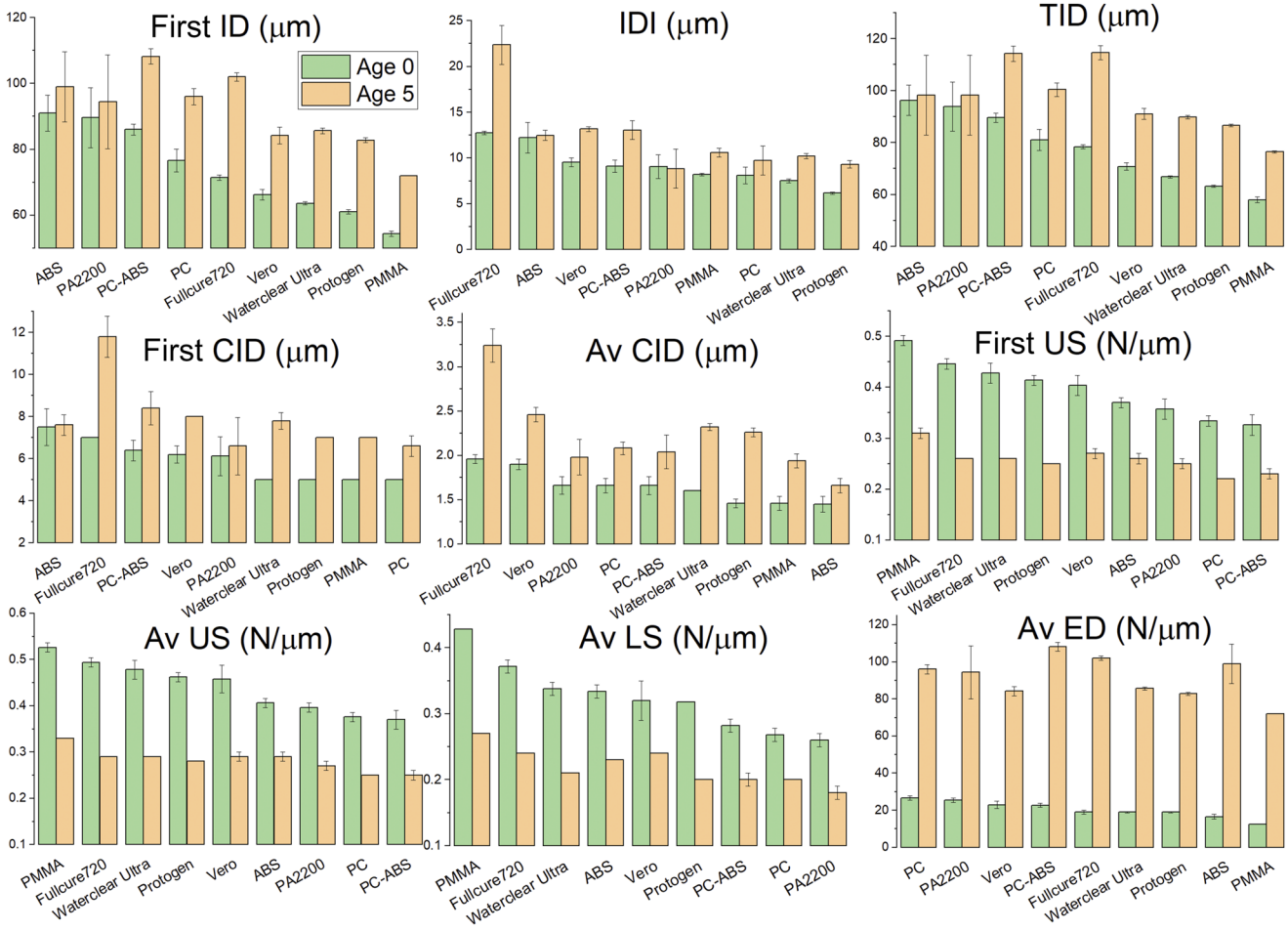

FIG. 3. BioDent nine parameter values of different polymers tested at Age 0 and Age 5. In each inset, polymers are sorted in descending order from left to right according to Age 0 values.

TABLE III. Mechanical properties of Age 0 and Age 5 polymers from tensile tests. Age 0 properties are collected from TechSheets. Age 5 properties are averaged using three measurements.

	Elastic modulus (GPa)		Ultimate stress (MPa)		Tensile elongation at break (%)	
	Age 0	Age 5	Age 0	Age 5	Age 0	Age 5
PA2200	1.68	0.61	48.70	44.03	18.70	20.29
Protogen	2.25	1.91	43.00	46.03	12.00	13.82
WaterClear Ultra	2.88	1.21	55.50	32.21	7.50	71.71
ABS	2.24	N/A	27.40	N/A	1.85	N/A
PC	2.03	0.64	38.50	27.40	2.15	6.34
Fullcure720	2.50	1.53	57.50	32.15	20.00	27.74
Vero	2.60	1.50	47.50	30.34	12.50	12.93
PMMA	2.86	N/A	75.00	N/A	4.50	N/A
PC-ABS	1.83	N/A	34.40	N/A	4.65	N/A
TangoBlack	N/A	N/A	2.00	0.34	47.70	109.78

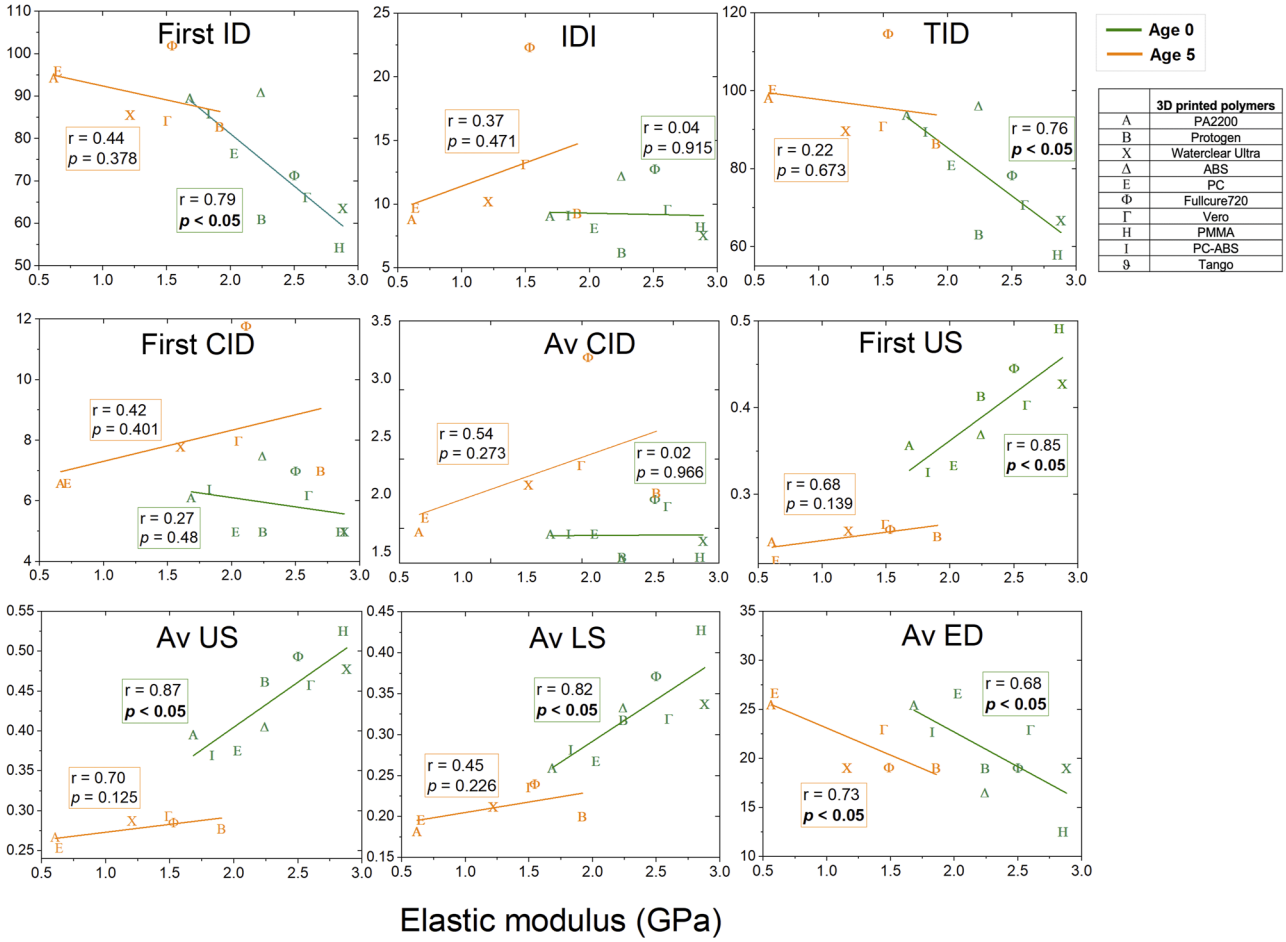

FIG. 4. Linear correlation between nine BioDent parameters and elastic modulus (GPa). Pearson's r and *p*-value (bolded for $p < 0.05$) are displayed next to each regression curve.

by tensile loading. The Age 0 tensile properties were collected from TechSheets from multiple sources. One-way ANOVA examined the statistical significance ($p < 0.05$) between BioDent parameters and mechanical properties. The same analysis was performed between BMSi and mechanical properties. Pearson's correlation coefficient r values were calculated for RPI parameters and mechanical properties to demonstrate the strength of the linear association between two variables.

III. RESULTS

BioDent and OsteoProbe tested Age 0 and Age 5 polymer samples. Nine parameters obtained from BioDent for different polymers are plotted in Fig. 3. In each subplot of Fig. 3, BioDent parameters are compared between Age 0 and Age 5 polymers. The polymers are sorted in each subplot in descending order from left to right according to Age 0 values to better visualize the properties of different materials. The BioDent data are unavailable for TangoBlack because it is too soft for the BP2 tip to apply the valid cyclic loading.

Among the Age 0 polymers, ABS-M30 has the largest first ID, TID, and first CID but the smallest Av CID. PMMA has the lowest first ID, TID, and Av ED. Its first CID and Av CID are also low. Meanwhile, PMMA has the highest first US, Av US, and Av LS. Following PMMA, FullCure720 has the second largest first US, Av US, and Av LS. However, unlike PMMA, which has a small Av CID, FullCure720 gets the largest Av CID, IDI, and large first CID. PC and PA2200 have large Av ED, which implies that this material can dissipate more energy during loading.

When we compare the parameters between Age 0 and Age 5, the polymers show significant property changes after aging, especially the Av ED, which increased around four times. The indentation distance parameters, including first ID, IDI, TID, first CID, and Av CID, increased after aging. On the contrary, the loading and unloading slope of Age 5 decreased to half of Age 0's. As the Age 0 polymers in each inset are sorted in descending order, we can easily see that the Age 5 polymers no longer follow the descending order.

The mechanical properties of Age 0 and Age 5 polymers, including elastic modulus, ultimate strength, and tensile elongation

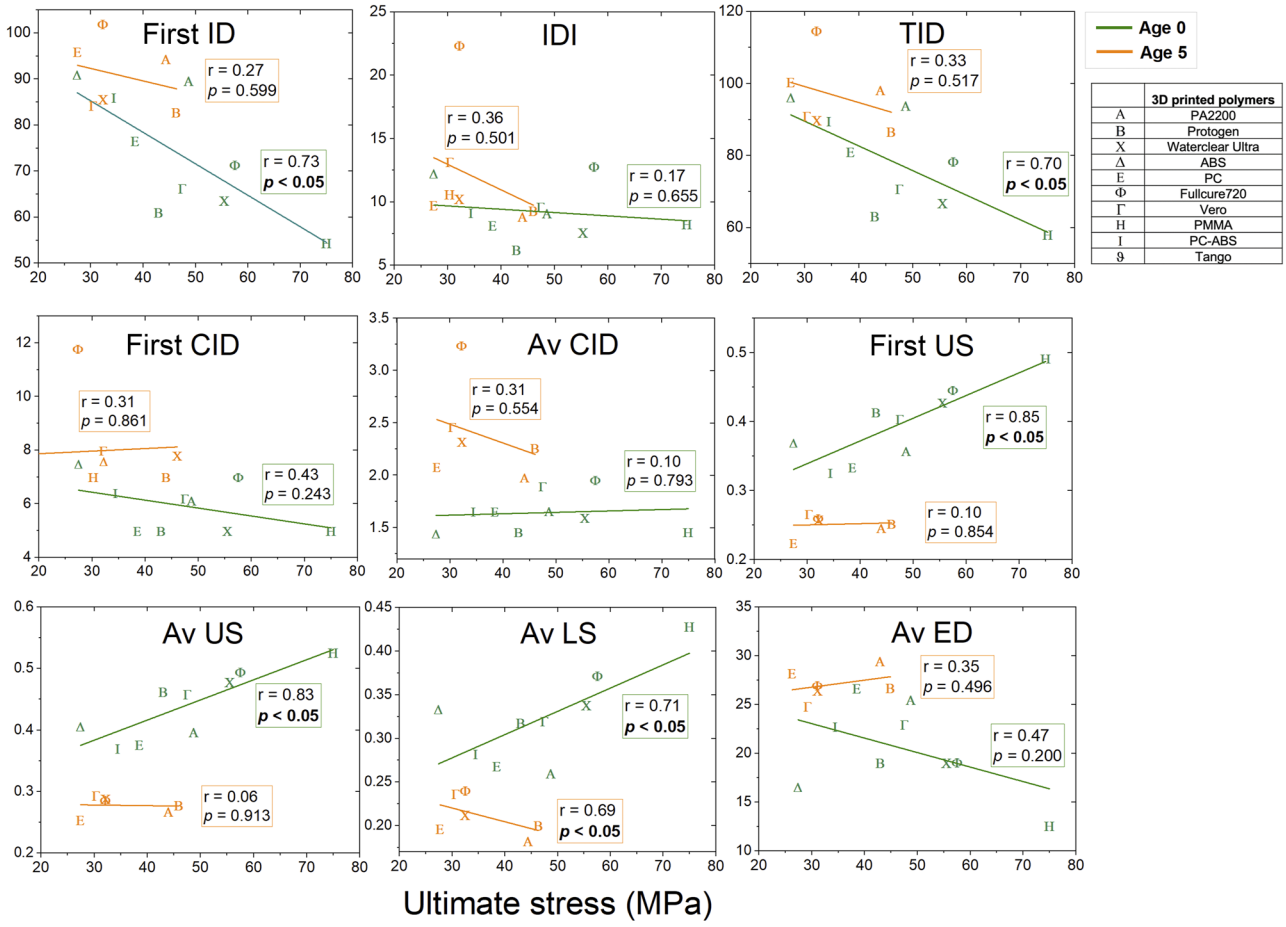

FIG. 5. Linear correlation between nine BioDent parameters and ultimate stress (MPa). Pearson's r and *p*-value (bolded for $p < 0.05$) are displayed next to each regression curve.

at break, are shown in Table III. Pearson's r values were calculated using linear regression for Age 0 and Age 5 polymers to correlate the RPI parameters with the mechanical properties. Nine RPI parameters from BioDent were correlated with the elastic modulus (Fig. 4), ultimate strength (Fig. 5), and tensile elongation at break (Fig. 6). BMSi from OsteoProbe was also correlated with these three mechanical properties in Fig. 7.

The correlations between BioDent parameters and mechanical properties are significant. For Age 0 polymers (green lines), the elastic modulus is highly correlated with the loading slope (r = 0.82) and unloading slope, including first US (r = 0.85) and AvUS (r = 0.87). The distance-related RPI parameters, first ID (r = 0.79) and TID (r = 0.76) correlate relatively highly with elastic modulus. For ultimate stress, first US and AvUS are still the most correlated parameters, whose r = 0.85 and 0.83, respectively, followed by Av LS with r = 0.71. First ID (r = 0.73) and TID (r = 0.70) also correlate relatively highly with the polymer's ultimate strength. Finally, the correlation between tensile elongation at break and RPI parameters is insignificant ($p > 0.05$). The most correlated parameter is AvCID with r = 0.60 ($p < 0.05$), and other RPI parameters have a correlation of r < 0.5 with elongation.

The linear regression curves for Age 5 polymers (orange lines) are plotted in the same figures as those of Age 0. After aging, the correlations between RPI parameters and mechanical properties become weaker. Av ED (r = 0.73) is the most correlated parameter to elastic modulus, followed by Av US (r = 0.70) and first US (r = 0.68). For correlation between RPI and ultimate stress, Av LS has r = 0.69, while other parameters have r < 0.5 and $p > 0.05$. Av US is the most correlated RPI parameter with Age 5 elongation (r = 0.45). None of the linear correlations between RPI and elongation is significant.

BMSi values were obtained from OsteoProbe for only Age 0 polymers. Figure 7 shows that BMSi is highly correlated with the elastic modulus (r = 0.85) and ultimate stress (r = 0.81). On the other hand, the correlation of BMSi with elongation is much lower, with r = 0.46 and $p > 0.05$, which exhibits no significance.

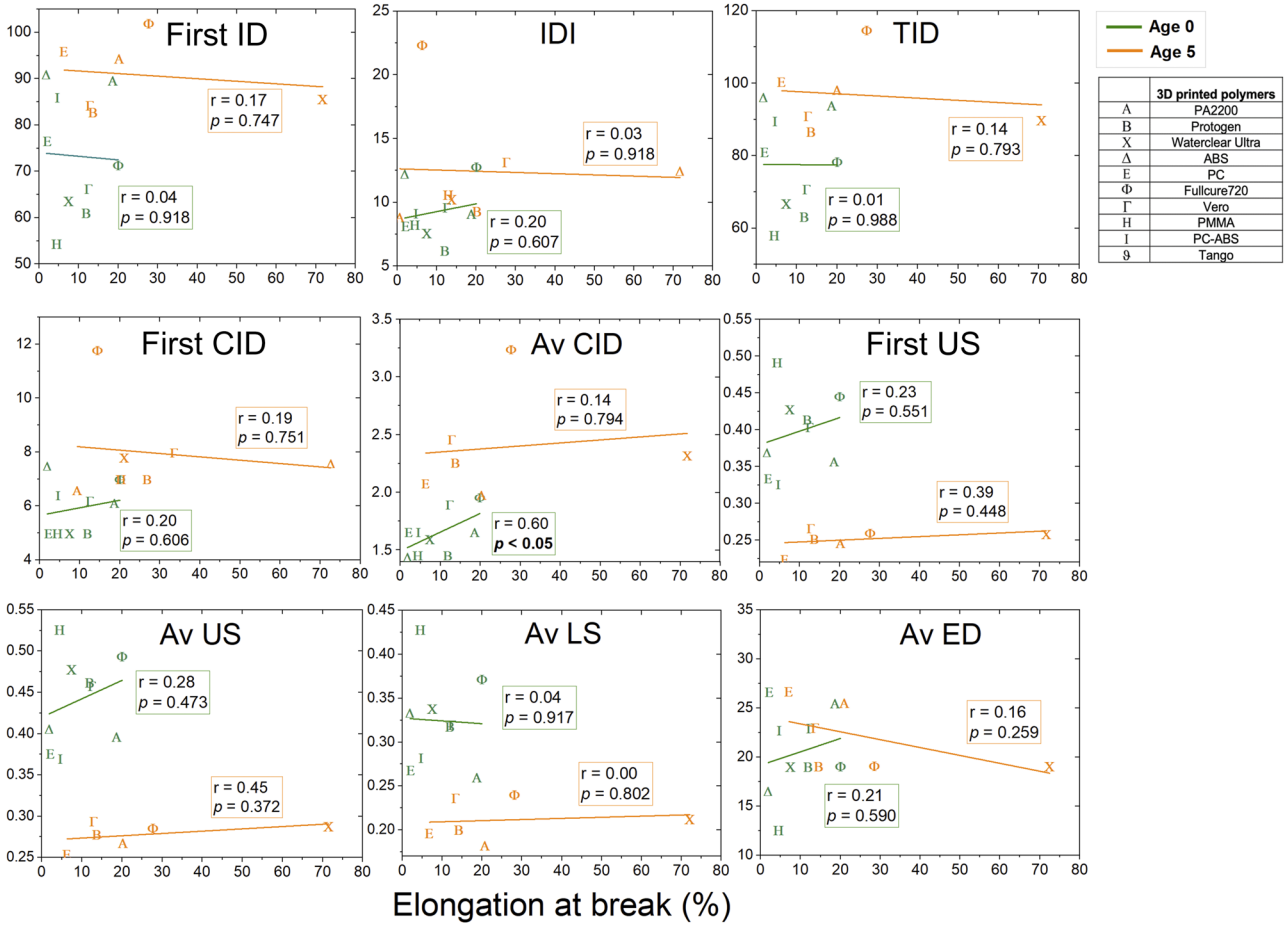

FIG. 6. Linear correlation between nine BioDent parameters and elongation at break (%). Pearson's r and *p*-value (bolded for $p < 0.05$) are displayed next to each regression curve.

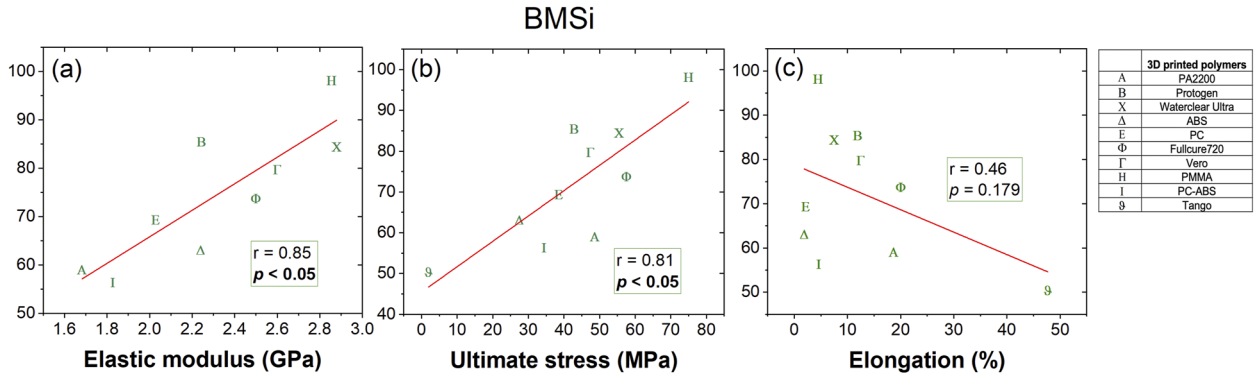

FIG. 7. Linear correlation between OsteoProbe parameters BMSi and (a) elastic modulus (GPa), (b) ultimate stress (MPa), and (c) elongation at break (%). Pearson's r and *p*-value (bolded for $p < 0.05$) are displayed next to the regression curve.

IV. DISCUSSION

This study performed reference point indentation tests using BioDent and OsteoProbe on nine 3D-printed polymers. Compared with traditional characterization techniques to obtain the mechanical properties from a stress–strain curve of polymers in a destructive way, RPI can derive a displacement–force curve with a straightforward setup while keeping the sample intact. The tensile test is a bulk measurement, while RPI is a localized surface measurement, and it can apply a cyclic loading with a much smaller tip size at a microscale. The indentation distance of the 3D-printed materials used in this study was within 0.12 mm. It is important to note that the printing layer thickness ranged from 0.02 to 0.35 mm, as indicated in Table II. Consequently, the indentation only occurred within a single layer or between multiple adjacent layers of the printed materials. Therefore, our findings demonstrate the correlation between the local properties obtained from cyclic loading using RPI and material's bulk properties.

ABS has the largest first CID, but its Av CID is the smallest among the studied polymers. Creep indentation distance measures the local resistance to fatigue.[25] Av CID is smaller than first CID for most materials because the material has been compressed in the iterative loadings. The significant difference between first CID and Av CID indicates that ABS has low plasticity and undergoes considerable strain hardening during the cyclic loading.

PMMA has very low indentation distance-related parameters such as first ID, TID, and CID, but its loading and unloading slopes are the highest. The loading and unloading slopes are stiffness-related parameters and measures of hardness, showing the ability to resist plastic deformation.[10,26] The energy dissipation of PMMA is also the lowest. Thus, of all these polymers, PMMA is the stiffest and hardest material that exhibits little plastic behavior.

FullCure720 ranks second in loading and unloading slopes, following the PMMA. However, unlike PMMA, FullCure720s first CID and Av CID are large. That means that FullCure720 is stiff, but it can creep.

To correlate RPI parameters with mechanical properties, Pearson's r was calculated for each RPI parameter in Figs. 4–7. For freshly printed polymers, the elastic modulus is significantly proportional to BMSi (r = 0.85), which is comparable to the study by Tang *et al.*,[18] who reported r = 0.98 between BMSi and elastic modulus from a tensile test on polymers. Elastic modulus is also highly proportionally correlated with the loading slope and first unloading slope with r = 0.82 and 0.85 because elastic modulus is identified at the linear region of the loading slope from the tensile stress–strain curve. However, Gallant *et al.*[10] obtained r = 0.44 between modulus and first US from rat bone, which shows less correlation. This result could be due to the inhomogeneity of the bone material. Sample properties may have larger variations as RPI performs localized indentation. Due to the limited study of RPI on polymers, most comparisons between our results are made with bone studies reported in the literature. Elastic modulus is inversely correlated with TID (r = 0.76) and Av ED (r = 0.68), which agrees with other studies[13,27] that concluded the inversely proportional correlation for bone. Total indentation distance and energy dissipation indicate plasticity, which is inversely proportional to modulus in most cases. Studies[13,28] showed that elastic modulus negatively correlates with IDI. However, that correlation in our result is extremely low, with r = 0.04, which barely shows any correlation.

Ultimate stress is another mechanical property that highly correlates with RPI parameters. Ultimate stress is proportionally correlated with BMSi (r = 0.81), first US (r = 0.85), Av US (r = 0.83), and Av LS (r = 0.71). Rasoulian[13] also showed a significant positive correlation between Av US and ultimate stress by studying age effects on porcine bones. More studies[10,13,27,29] found that ultimate stress and yield stress of bone materials are negatively correlated with TID, which agrees with our results. Gallant *et al.*[10] reported a correlation of ultimate stress with TID and first ID obtained from bone tests as r = 0.48 and 0.36, respectively, smaller than ours (r = 0.70 and 0.73, respectively). The main reason could be again due to the inhomogeneity of bone structure.

Finally, the correlations calculated between elongation and RPI parameters are insignificant except between elongation and Av CID r = 0.6 ($p < 0.05$). Polymer's elongation at break is sensitive to multiple factors such as the tensile strain rate during testing, printing and loading directions, polymer's crystallinity and cross-linking density, and temperature. Yet, RPI performs indents on a microscale, which may not reflect the bulk elongation trend. Elongation of polymers

may display significance at a larger scale due to the long molecular chains.

Brostow and Zhang[30] showed that a tensile elongation at the break of polymers has a strong correlation (r^2 = 0.821) with Vickers hardness, which uses a much larger tip to perform indentation. A comparison study using Vickers hardness, RPI, and nanoindentation could reveal a better correlation to examine the correlation between RPI and elongation at break.

Compared to Age 0 polymers, the Age 5 polymers have lower elastic modulus, lower ultimate stress, and higher elongation. Polymer aging, involving changes with time, is a complex process. Polymer aging may include physical, chemical, thermal changes, photochemical changes, or a combination.[21] Many factors, such as temperature, moisture, ultraviolet light, and weathering, can lead to aging. Furthermore, curing temperature and degree of crystallinity can influence aging. 3D printers deposit layers additively, and the fast cooling during printing may cause high-temperature gradients, leading to high residual stresses. Residual stress has a substantial impact on the mechanical properties. Over five years, stresses may be partially relieved due to physical aging that involves molecular relaxations.[31] In addition, samples were placed on a shelf in the lab where the temperature was controlled at 20 °C, but they occasionally were exposed to indoor lighting.

We assume that the main reasons for the studied polymers' aging were physical aging and photo aging. The chosen 3D-printed polymers are all amorphous materials except for PA2200, which is semi-crystalline. Secondary crystallization might have occurred in the amorphous region. It could be further accelerated by the chain scission by photo aging, causing residual stress in the polymer and leading to low mechanical properties.

We also observed that the correlations between the RPI parameters and mechanical properties became insignificant for Age 5 polymers. The significant property changes of Age 5 polymers may be due to the material properties varying along the sample depth profile due to photo aging and oxidation. Under photo aging, the sample surface would suffer heavier molecular degradation and other changes along the sample depth profile.[32,33]

Studies investigating the aging of 3D printed polymers generally have focused on accelerated aging due to temperature, moisture, or radiation.[5,24,25] In a study most closely related to our work, Bochnia[26] tested in tension two 3D printed polymers, VeroWhite and FullCure720, at Age 0 and eight years after storage in the laboratory. He reported significant changes in the elastic modulus and tensile strength as a function of age and printing orientation.

This study has several limitations. Including more samples with a broader range of polymer properties could give better linear correlations. In addition, we took the tensile properties from TechSheets on 3D-printed polymers at Age 0. While we observed similar properties in our study compared to the tensile test measurements conducted on Age 0 polymers in our lab, it is important to note that our comparison was based on results from only one sample for each polymer type. This limited sample size may introduce variability and potential bias in the findings. In addition, it is worth mentioning that the OsteoProbe device was not available during Year 5 of our study. As a result, we could not present Age 5 OsteoProbe results in our analysis.

In this study, we compared the RPI results with the tensile properties of polymers while the RPI applies compressive loadings. We used the tensile test results for two main reasons. Material manufacturers typically list the tensile properties of polymers in their datasheets. Second, the ultimate tensile strength of polymers is challenging to interpret due to strain hardening. Future studies could investigate the correlations of the RPI results with compressive test results to better understand the RPI outputs.

Furthermore, it should be noted that we purchased the 3D-printed materials used in this study from a commercial lab, and thus, there was limited control over the printing parameters. A more detailed investigation into the sample processing could be explored in future studies to enhance further the understanding and control of the 3D-printed material properties.

Regarding the aged samples, prolonged exposure to the atmosphere may result in surface aging effects. To gain deeper insights into the aged samples, future study could employ the RPI technique by cutting the sample in half and conducting measurements on those newly opened surfaces. This approach would help minimize the influence of indentation on the oxidized surface, enabling a more focused analysis of the internal properties of the material. Such experiments would allow for deeper understanding of polymer aging.

V. CONCLUSIONS

Reference point indentation (RPI) is a nondestructive technique that can apply cyclic microindents on the sample surface. The RPI parameters obtained from BioDent (nine parameters) and OsteoProbe (BMSi) were linearly correlated with the mechanical properties determined from tensile tests to understand better how the RPI outputs relate to polymer properties. Measurements were performed on nine distinct 3D-printed polymers. Only correlations that achieved statistical significance ($p < 0.05$) were considered. For the Age 0 polymers, the elastic modulus is highly correlated with Av unloading slope (r = 0.87), first unloading slope (r = 0.85), BMSi (r = 0.85), loading slope (r = 0.82), first ID (r = 0.79), and TID (r = 0.76). Ultimate stress is mostly correlated with first unloading slope (r = 0.85), Av unloading slope (r = 0.83), BMSi (r = 0.81), ID (r = 0.73), Av loading slope (r = 0.71), first and TID (r = 0.70). The most correlated RPI parameter to elongation at break is Av CID with r = 0.60. In addition to the study of Age 0 polymers, Age 5 polymers were found to have changed mechanical properties and were less correlated with the RPI parameters. This study demonstrates the potential of RPI to assess the mechanical properties of polymers nondestructively. Furthermore, for the first time, 3D-printed polymers and aged polymers were investigated with RPI.

ACKNOWLEDGMENTS

This research has been supported by the National Science Foundation Center for Novel High Voltage/Temperature Materials and Structures (Grant No. IIP-1362146) and the National Science Foundation Mechanics of Materials and Structures program (Grant No. CMMI-1926353). The findings, conclusions, and recommendations expressed in this manuscript are those of the authors and do not necessarily reflect the views of the NSF.

AUTHOR DECLARATIONS

Conflict of Interest

The authors have no conflicts to disclose.

Author Contributions

Siyuan Pang: Data curation (equal); Formal analysis (equal); Investigation (equal); Methodology (equal); Validation (equal); Visualization (equal); Writing – original draft (lead); Writing – review & editing (equal). **Iwona Jasiuk**: Conceptualization (lead); Funding acquisition (lead); Investigation (equal); Methodology (equal); Project administration (lead); Resources (lead); Supervision (lead); Writing – review & editing (equal).

DATA AVAILABILITY

The data that support the findings of this study are available from the authors upon reasonable request.

REFERENCES

[1] P. K. Hansma, P. J. Turner, and G. E. Fantner, "Bone diagnostic instrument," Rev. Sci. Instrum. **77**(7), 075105 (2006).

[2] P. Hansma, P. Turner, B. Drake, E. Yurtsev, A. Proctor, P. Mathews, J. Lelujian, C. Randall, J. Adams, and R. Jungmann, "The bone diagnostic instrument II: Indentation distance increase," Rev. Sci. Instrum. **79**(6), 064303 (2008).

[3] C. Randall, D. Bridges, R. Guerri, X. Nogues, L. Puig, E. Torres, L. Mellibovsky, K. Hoffseth, T. Stalbaum, A. Srikanth *et al.*, "Applications of a new handheld reference point indentation instrument measuring bone material strength," J. Med. Devices **7**(4), 041005 (2013).

[4] Active Life Scientific, BioDent Calculations, 2021.

[5] D. Bridges, C. Randall, and P. K. Hansma, "A new device for performing reference point indentation without a reference probe," Rev. Sci. Instrum. **83**(4), 044301 (2012).

[6] J. N. Farr, M. T. Drake, S. Amin, L. J. Melton III, L. K. McCready, and S. Khosla, "In vivo assessment of bone quality in postmenopausal women with type 2 diabetes," J. Bone Miner. Res. **29**(4), 787–795 (2014).

[7] J. R. Furst, L. C. Bandeira, W.-W. Fan, S. Agarwal, K. K. Nishiyama, D. J. McMahon, E. Dworakowski, H. Jiang, S. J. Silverberg, and M. R. Rubin, "Advanced glycation endproducts and bone material strength in type 2 diabetes," J. Clin. Endocrinol. Metab. **101**(6), 2502–2510 (2016).

[8] L. Mellibovsky, D. Prieto-Alhambra, F. Mellibovsky, R. Güerri-Fernández, X. Nogués, C. Randall, P. K. Hansma, and A. Díez-Perez, "Bone tissue properties measurement by reference point indentation in glucocorticoid-induced osteoporosis," J. Bone Miner. Res. **30**(9), 1651–1656 (2015).

[9] M. R. Allen, E. M. B. McNerny, J. M. Organ, and J. M. Wallace, "True gold or pyrite: A review of reference point indentation for assessing bone mechanical properties in vivo," J. Bone Miner. Res. **30**(9), 1539–1550 (2015).

[10] M. A. Gallant, D. M. Brown, J. M. Organ, M. R. Allen, and D. B. Burr, "Reference-point indentation correlates with bone toughness assessed using whole-bone traditional mechanical testing," Bone **53**(1), 301–305 (2013).

[11] G. H. Yassen, T.-M. G. Chu, M. A. Gallant, M. R. Allen, M. M. Vail, P. E. Murray, and J. A. Platt, "A novel approach to evaluate the effect of medicaments used in endodontic regeneration on root canal surface indentation," Clin. Oral Invest. **18**, 1569–1575 (2014).

[12] A. Chang, G. W. Easson, and S. Y. Tang, "Clinical measurements of bone tissue mechanical behavior using reference point indentation," Clin. Rev. Bone Miner. Metab. **16**, 87–94 (2018).

[13] R. Rasoulian, A. Raeisi Najafi, M. Chittenden, and I. Jasiuk, "Reference point indentation study of age-related changes in porcine femoral cortical bone," J. Biomech. **46**(10), 1689–1696 (2013).

[14] M. J. Olszta, X. Cheng, S. S. Jee, R. Kumar, Y.-Y. Kim, M. J. Kaufman, E. P. Douglas, and L. B. Gower, "Bone structure and formation: A new perspective," Mater. Sci. Eng.: R: Rep. **58**(3–5), 77–116 (2007).

[15] L. Marsavina, A. Cernescu, E. Linul, D. Scurtu, and C. Chirita, "Experimental determination and comparison of some mechanical properties of commercial polymers," Mater. Plast. **47**(1), 85–89 (2010).

[16] N. Saba, M. Jawaid, and M. T. H. Sultan, "An overview of mechanical and physical testing of composite materials," in *Mechanical and Physical Testing of Biocomposites, Fibre-Reinforced Composites and Hybrid Composites* (Woodhead Publishing, 2019), pp. 1–12.

[17] F. S. Ly, A. Proctor, K. Hoffseth, H. T. Yang, and P. K. Hansma, "Significant correlation of bone material strength index as measured by the O with Vickers and Rockwell hardness," Rev. Sci. Instrum. **91**(8), 084102 (2020).

[18] S. Y. Tang, P. Mathews, C. Randall, E. Yurtsev, K. Fields, A. Wong, A. C. Kuo, T. Alliston, and P. Hansma, "*In situ* materials characterization using the tissue diagnostic instrument," Polym. Test. **29**(2), 159–163 (2010).

[19] I. Jasiuk, D. W. Abueidda, C. Kozuch, S. Pang, F. Y. Su, and J. McKittrick, "An overview on additive manufacturing of polymers," JOM **70**(3), 275–283 (2018).

[20] J. S. Saini, L. Dowling, J. Kennedy, and D. Trimble, "Investigations of the mechanical properties on different print orientations in SLA 3D printed resin," Proc. Inst. Mech. Eng., Part C **234**(11), 2279–2293 (2020).

[21] C. G. Amza, A. Zapciu, F. Baciu, M. I. Vasile, and A. I. Nicoara, "Accelerated aging effect on mechanical properties of common 3D-printing polymers," Polymers **13**(23), 4132 (2021).

[22] D. W. Abueidda, M. Elhebeary, C.-S. A. Shiang, S. Pang, R. K. Abu Al-Rub, and I. M. Jasiuk, "Mechanical properties of 3D printed polymeric Gyroid cellular structures: Experimental and finite element study," Mater. Des. **165**, 107597 (2019).

[23] Stratasys, Safety Data Sheets, 2017.

[24] A. Setters and I. Jasiuk, "Towards a standardized reference point indentation testing procedure," J. Mech. Behav. Biomed. Mater. **34**, 57–65 (2014).

[25] A. Carriero, J. L. Bruse, K. J. Oldknow, J. L. Millán, C. Farquharson, and S. J. Shefelbine, "Reference point indentation is not indicative of whole mouse bone measures of stress intensity fracture toughness," Bone **69**, 174–179 (2014).

[26] M. Granke, A. Coulmier, S. Uppuganti, J. A. Gaddy, M. D. Does, and J. S. Nyman, "Insights into reference point indentation involving human cortical bone: Sensitivity to tissue anisotropy and mechanical behavior," J. Mech. Behav. Biomed. Mater. **37**, 174–185 (2014).

[27] A. Idkaidek, V. Agarwal, and I. Jasiuk, "Finite element simulation of reference point indentation on bone," J. Mech. Behav. Biomed. Mater. **65**, 574–583 (2017).

[28] C. Randall, P. Mathews, E. Yurtsev, N. Sahar, D. Kohn, and P. Hansma, "The bone diagnostic instrument III: Testing mouse femora," Rev. Sci. Instrum. **80**(6), 065108 (2009).

[29] M. A. Hammond, M. A. Gallant, D. B. Burr, and J. M. Wallace, "Nanoscale changes in collagen are reflected in physical and mechanical properties of bone at the microscale in diabetic rats," Bone **60**, 26–32 (2014).

[30] W. Brostow and D. Zhang, "Tensile elongation at break for polymers related to Vickers hardness," Mater. Lett. **276**, 128179 (2020).

[31] J. R. White, "Polymer ageing: Physics, chemistry or engineering? Time to reflect," C. R. Chim. **9**(11–12), 1396–1408 (2006).

[32] B. Haworth, G. J. Sandilands, and J. R. White, "Characterization of injection moulding," Plast. Rubber Int. **5**(3), 109–113 (1980).

[33] I. M. Cuckson, B. Haworth, G. J. Sandilands, and J. R. White, "Internal stress assessment of thick-section injection-mouldings," Int. J. Polym. Mater. Polym. Biomater. **9**(1), 21–36 (1981).